Characterization and Analysis of Seismic Signals from the February 4th, 2025 Perforation Gun-Firing at OGDCL Soghri Well (Rig-215)

Author: Mr. Nasir Mahmood, Meteorologist, Qamar Hussain, Electronic Engineer

Supervised By: Dr. Muhammad Afzaal, Chief Meteorologist, Najeeb Ahmed Amir, Director

Pakistan Meteorological Department, Islamabad (*March, 2025*)

Table of Contents

Characterization and Analysis of Seismic Signals from the February 4th, 2025 Perforation Gun-Firing at OGDCL Soghri Well (Rig-215)

By Nasir Mahmood *(Meteorologist)* and Qamar Hussain *(Electronic Engineer)*

Seismic Monitoring Center, Pakistan Meteorological Department, H-8/2, Islamabad, Pakistan.

Abstract

This study investigates the induced seismicity caused by perforation gun firing at the OGDCL Soghri Well (Rig-215) in Attock, Pakistan, on February 4, 2025. Short-period seismometers were deployed at distances of 30m, 500m, and 1500m from the well to monitor seismic activity. Micro-earthquakes with magnitudes of Mw 1.4, 0.8, and 1.1, characterized by high-frequency vibrations, were detected at the nearest site, indicating the seismic impact of the perforation. Data from more distant sites proved challenging due to low signal-to-noise ratios, energy attenuation, and interference from anthropogenic noise. The perforation gun signal, differing from natural earthquakes, overlapped with noise but revealed the seismic impact at the well site. Ground shaking associated with the induced seismicity raised concerns, especially regarding potential risks to surrounding infrastructure. Ground motion estimates based on an empirical model indicated peak ground acceleration (PGA) of 0.01 to 0.151 cm/s² near the epicenter, with weaker motion at farther sites. These results align with seismic waveform analysis. The study underscores the importance of understanding local geology, fault systems, and integrating seismic monitoring with well data to mitigate induced seismicity risks. Recommendations include deploying broadband seismometers, expanding sensor arrays, and using advanced signal processing to improve detection accuracy.

1. Introduction

Induced seismicity resulting from perforation gun firing in deep oil and gas wells is a crucial consideration for monitoring the integrity of reservoir dynamics and mitigating potential geo-hazards. Present work focuses on seismic monitoring during perforation activities at a depth of 4500 meters at the OGDCL Soghri Well, located in Attock, Pakistan. The primary objective of the study is to analyze seismic signals, assess induced seismicity, and understand ground shaking effects associated with perforation gun firing.

Seismic monitoring at such depths poses challenges, including significant signal attenuation, poor signal-to-noise ratios (SNR), and limited spatial coverage. This assesses these challenges and investigates potential solutions to improve seismic monitoring capabilities for deep reservoir operations.

1.1 Background of Study:

During the early phase of drilling at the Soghri Well in May 2024, micro-seismic events with magnitudes ranging from 0.2 to 0.8 were detected at a depth of 120 meters. The perforation gun firing at 4500 meters in February 2025, however, posed a more significant seismic risk, warranting comprehensive monitoring. Seismological data was collected by three short-period seismometers placed at 30 meters, 500 meters, and 1500 meters from the well. The aim was to understand how perforation-induced seismicity propagates in the surrounding sedimentary region and the intensity of ground shaking resulting from the perforation process.

Figure 1: OGDCL Soghri Well Site, highlighting the hydraulic drilling and perforation area at the center (red circle).

2. Methodology

Seismic monitoring was carried out using three short-period seismometers placed at different distances from the perforation site (30m, 500m, and 1500m). The sensors recorded seismic waveforms, including high-frequency vibrations, which were then processed with advanced techniques such as band-pass filtering to eliminate unwanted frequencies and noise, Fourier Transform (FFT) for frequency domain analysis of the seismic signals, and Wavelet Analysis for time-frequency decomposition of the waveforms. Moment Magnitude (Mw) was estimated using the peak displacement method, where seismic moments were derived from the displacement

records. Micro-earthquake magnitudes were also calculated using both local magnitude (Ml) and moment magnitude (Mw) scales.

The Nakamura technique using geopsy tool was applied to evaluate background noise levels (noise PSD), H/V estimate and a ground shaking map was created using empirical relations to assess the spatial extent and impact of induced seismicity caused by the perforation process at the well.

2.1 Sensor Deployment:

Three seismometers were placed at the following locations:

- **Site 1**: 30 meters from the perforation gun, positioned on a flat surface near the well.
- **Site 2**: 500 meters away, located in a sedimentary area with alluvial deposits.
- **Site 3**: 1500 meters from the well, also situated in a loose sedimentary region.

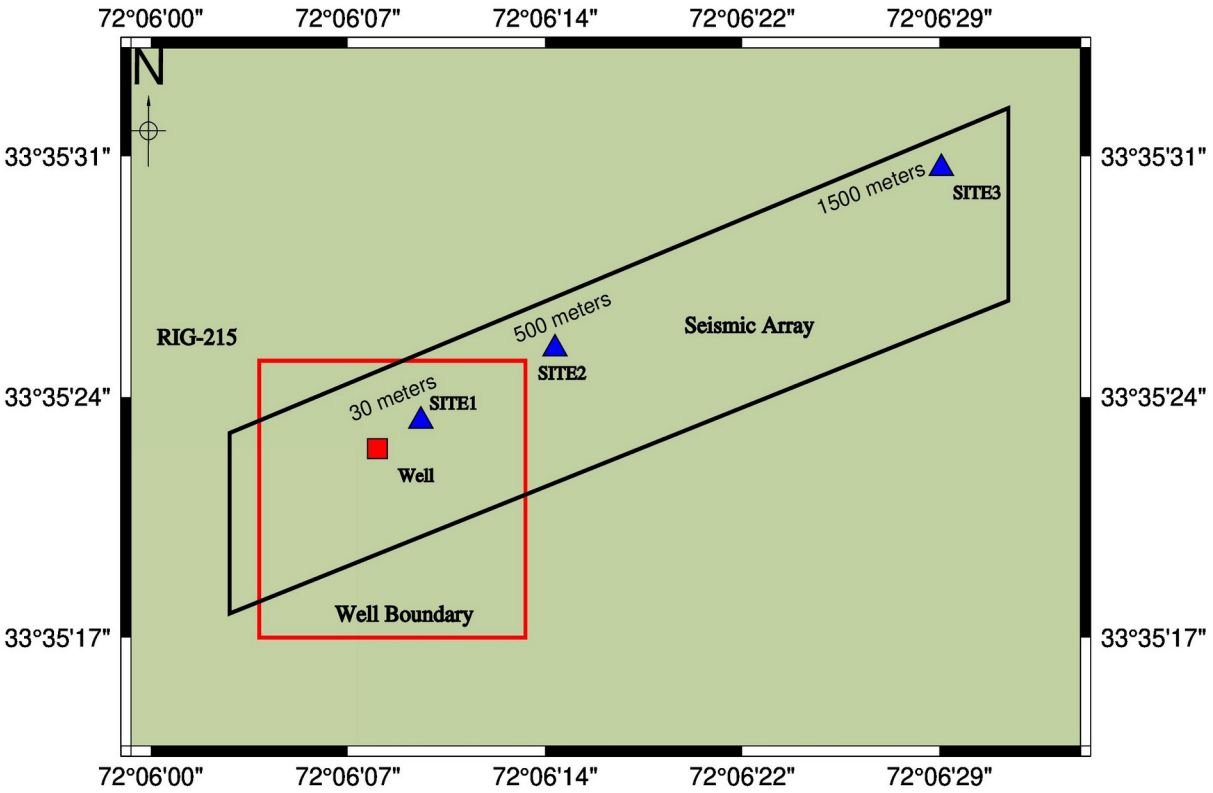

Figure 2: Seismic array deployment with three GPL20 sensors (blue triangles) at Site 1 (30 m), Site 2 (500 m), and Site 3 (1500 m). The well area is indicated by a red square, and the well boundary is outlined.

Figure 3: GL-PS2 short-period sensors used as seismic monitoring instruments in the present study.

Figure 4a: View of the soft sedimentary alluvium area where seismic monitoring was conducted during perforation gun firing.

Figure 4b: View of sites outside the well boundary: Site 2 (500m) and Site 3 (1500m), with the rig tower in the background. These sites were located in areas with loose sedimentary alluvium.

2.2 Seismic Waveform Data Analysis:

The seismic events induced by perforation gun fire are typically small in magnitude, often categorized as microseismic or low-magnitude events. However, their frequency can vary based on factors such as reservoir size, the number of perforation shots, and local geological conditions. These seismic events are generally short-lived and remain localized around the wellbore.

In the present experiment, seismic signals, including high-frequency vibrations, were recorded during the perforation event and processed using SAC (Goldstein, 2005), Seisan 13 (Ottemöller, 2021) and ObsPy tools. Techniques like band-pass filtering, Fourier Transform, and wavelet analysis were applied. Micro-earthquake magnitudes were estimated, background noise assessed using Nakamura technique, and a ground shaking map is constructed to evaluate seismic impacts at three sites.

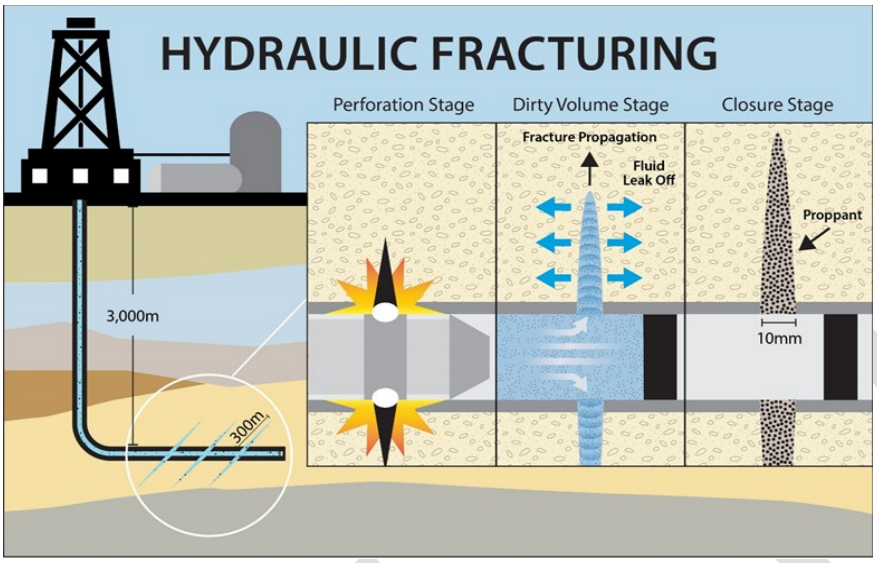

Figure 5: Schematic diagram illustrating the stages of hydraulic fracturing, including perforation, fluid injection, and well production. *Courtesy: web source.*

Figure 6: Specialized vehicle equipped with a slick-line unit used to discharge the perforation gun inside the wellbore on February 4, 2025, at 03:02:55 GMT.

2.3 Micro-earthquake Detection:

During the perforation process, clear micro-events were detected, with seismic signals most pronounced at Site 1. Minor peaks were observed at Sites 2 and 3, but due to signal attenuation and poor SNR, it was unclear whether these were micro-seismic events or just noise.

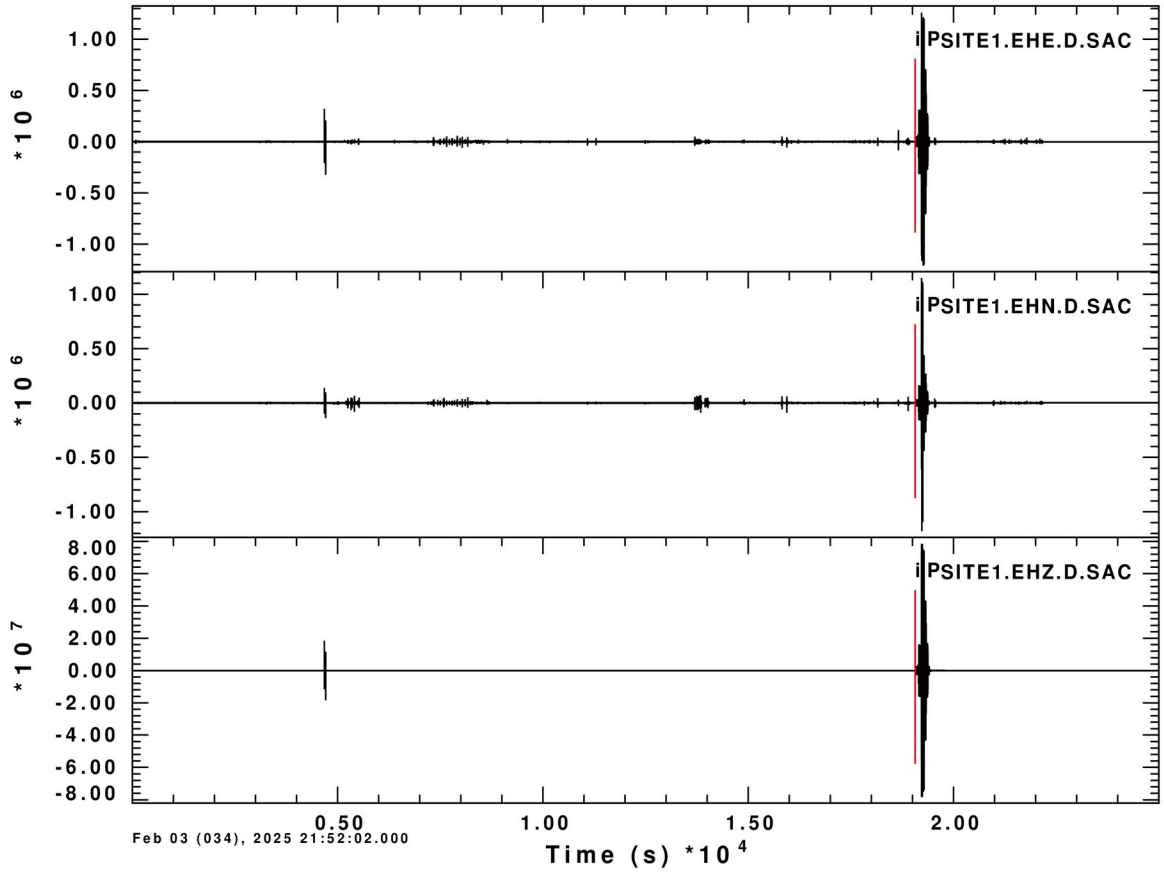

Figure 7: Micro-seismic activity triggered by perforation gun fire at OGDCL Well, detected on February 4, 2025, at 03:03:02 GMT, with a distinct peak highlighted by a red marker on the continuous time series data. The recording at Site 1 began on February 3, 2025, around 21:50 GMT.

Short-period seismometers at 30, 500, and 1500 meters detected seismic signals, particularly at Site1, where micro-earthquakes with high-frequency vibrations highlighted the perforation's seismic impact. The rapid energy release from perforation detonation drives these events. The high-frequency, short-duration waves of the perforation signal differ from natural earthquakes

but overlap with anthropogenic noise. These localized, short-lived events are influenced by reservoir size, shot frequency, and local geology, and may trigger further activity if reservoir pressure increases or faults reactivate.

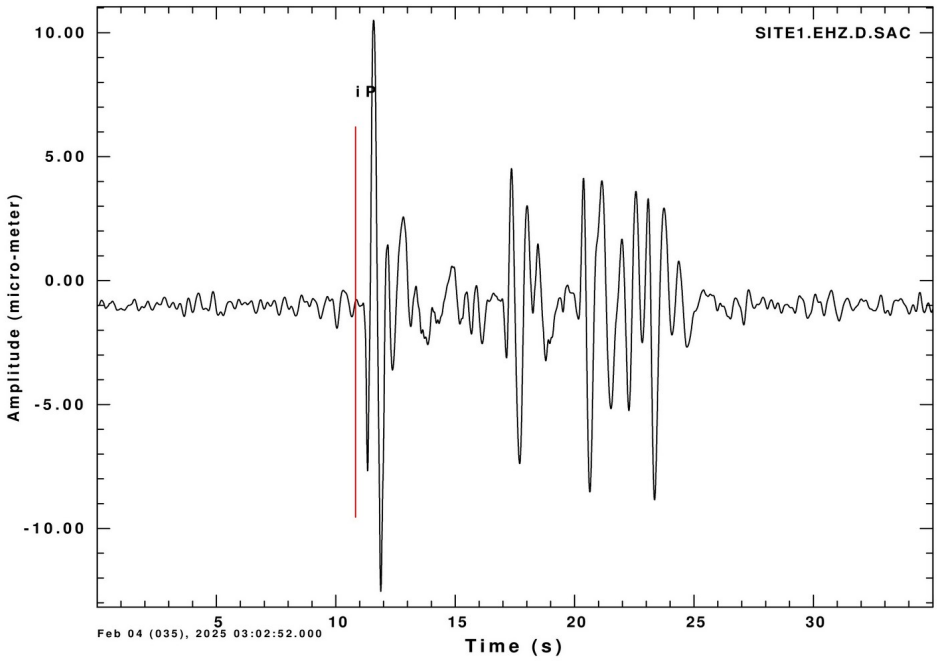

Figure 8: Seismic signals from a micro-earthquake with distinct peaks and high signal-to-noise ratio (SNR), detected by a sensor located 30 meters from the well.

3. Results

3.1 Moment Magnitude (Mw) Estimate:

Moment Magnitude (Mw) was estimated using the peak displacement from the SAC file, converted from velocity to displacement via integration. The peak displacement (in micrometers) was used to calculate seismic moment (M_O) using an empirical formula and Mw was computed using the Kanamori (1977) relation (eq. 1).

$$Mw = 2/3 \log10 (M_0) - 10.7 \qquad \text{(eq.1)}$$

The seismic signals from the perforation event revealed micro-earthquakes with magnitudes ranging from 0.2 to 1.4, with the strongest (Mw 1.4) detected at Site 1 (30 meters). Signals were

most prominent at Site 1, with weaker signals at Sites 2 and 3 due to attenuation and poor SNR. The perforation gun at 4500 meters caused rock fracturing, generating small-magnitude events, mainly detected at Site 1.

3.1.1 SAC-Waveform Processing Steps:

```
SAC> r SITE1.EHZ.D.SAC
SAC> rmean
SAC> rtrend
SAC> bp c 0.1 5 (BP: corners fl 0.100000 fh 5.000000 npoles 1 pass 1 Butterworth)
SAC> integrate
SAC> w append
SITE1.EHZ.D.SAC
SAC> markptp
```

Using SAC code, the instrument response was removed from the seismic data by applying the RESP file for the Z-channel, correcting for instrumental noise and allowing an accurate estimate of ground motion. After this correction, the peak displacement of the micro-earthquake was calculated to be approximately 12.1µm, representing the maximum vertical displacement recorded by the sensor at Site 1.

3.1.2 Python tool obspy Processing Steps:

```
>>> from math import log10

>>> peak displacement = 12.1

>>> M0 = 10** (1.5 * 12.1)

>>> Mw = (2 / 3) * log10 (M0) - 10.7

>>> print (f "Moment Magnitude  (Mw): {Mw}" )

Moment Magnitude (Mw): 1.399

>>> Mw= 1.4
```

3.2 Spectrogram Analysis:

The spectrogram of the seismogram recorded at Site1 near the OGDCL well during perforation gun firing on February 4, 2025, at 03:03 GMT reveals high-frequency vibrations associated with micro-earthquakes, confirming the occurrence of micro-seismicity. The analysis identified three distinct peaks, corresponding to micro-earthquakes with magnitudes of Mw 1.4**,** Mw 0.8, and Mw 1.1. These events were triggered by the perforation at a depth of 4500 meters, with the rapid

energy release from the perforation detonation driving the seismic activity. The spectrogram shows time on the x-axis, frequency (Hz) on the y-axis, and signal power represented by color.

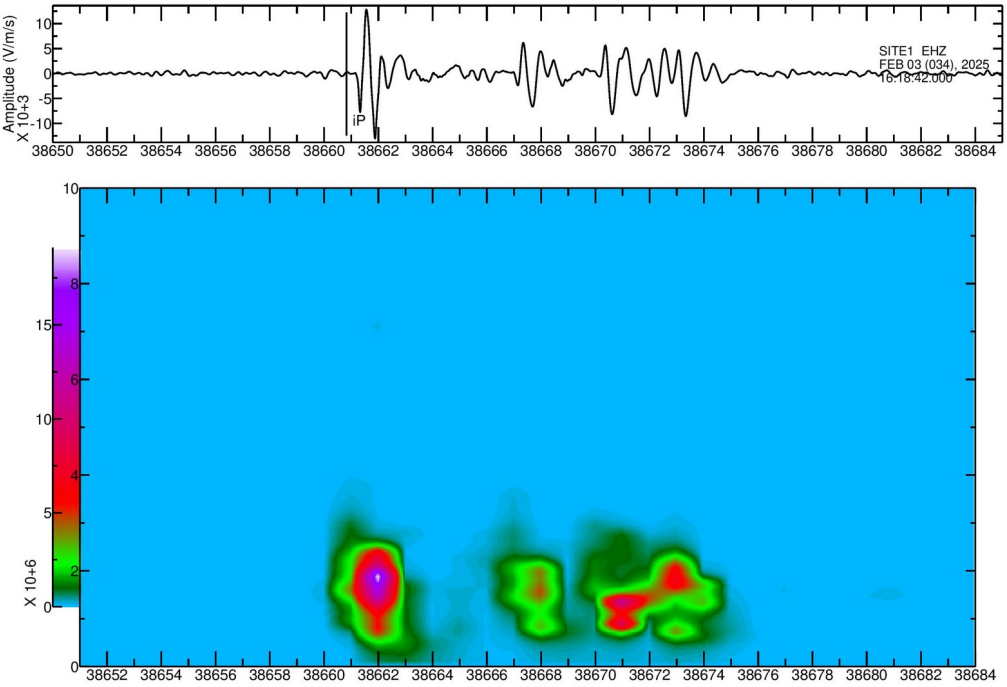

Figure 9: Spectrogram analysis revealing high-frequency vibrations corresponding to prominent micro-earthquakes with magnitudes Mw 1.4 and Mw 1.1.

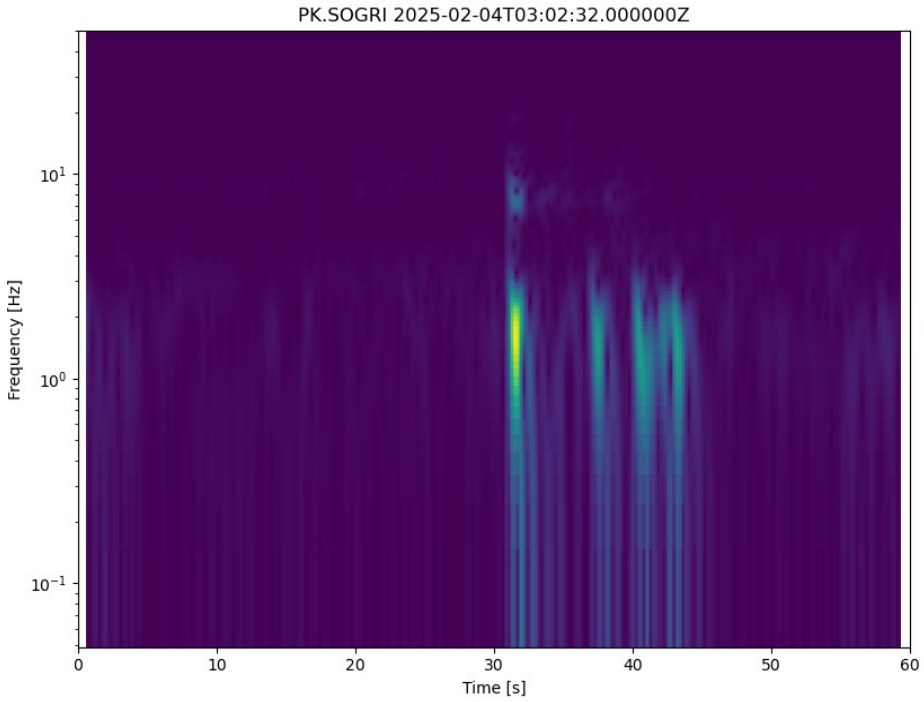

Figure 9a: Spectrogram revealing high-frequency vibrations corresponding to the micro-earthquake activity detected at the nearest site.

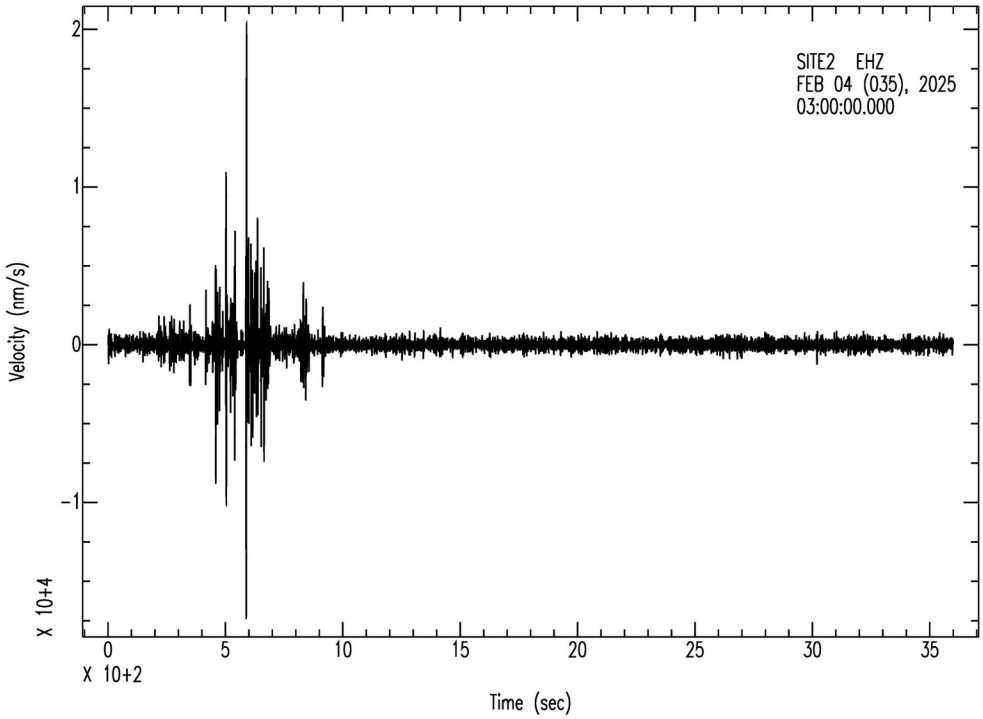

Figure 10: Seismic signals detected at Site 2, located 500 meters from the well, during perforation gunfire.

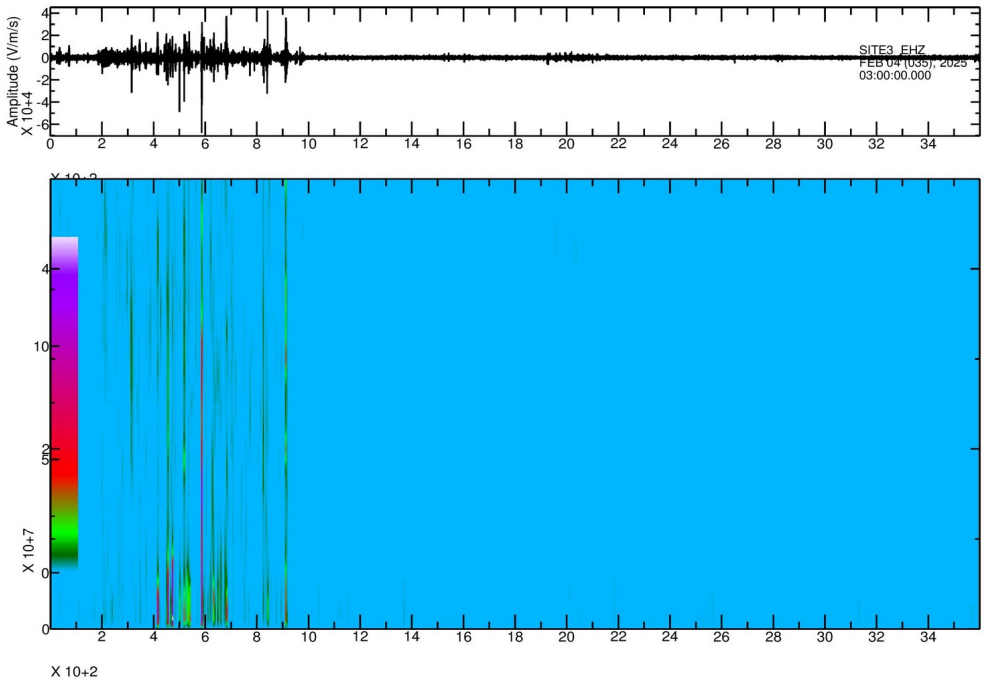

Figure 10a: Spectrogram analysis of the seismic waveform revealing high-frequency vibrations corresponding to the perforation gunfire, recorded at Site 2, 500 meters from the well.

At 500-meter and 1500-meter distances from the well, considerable signal attenuation and low SNR make it difficult to detect seismic events amidst background noise.

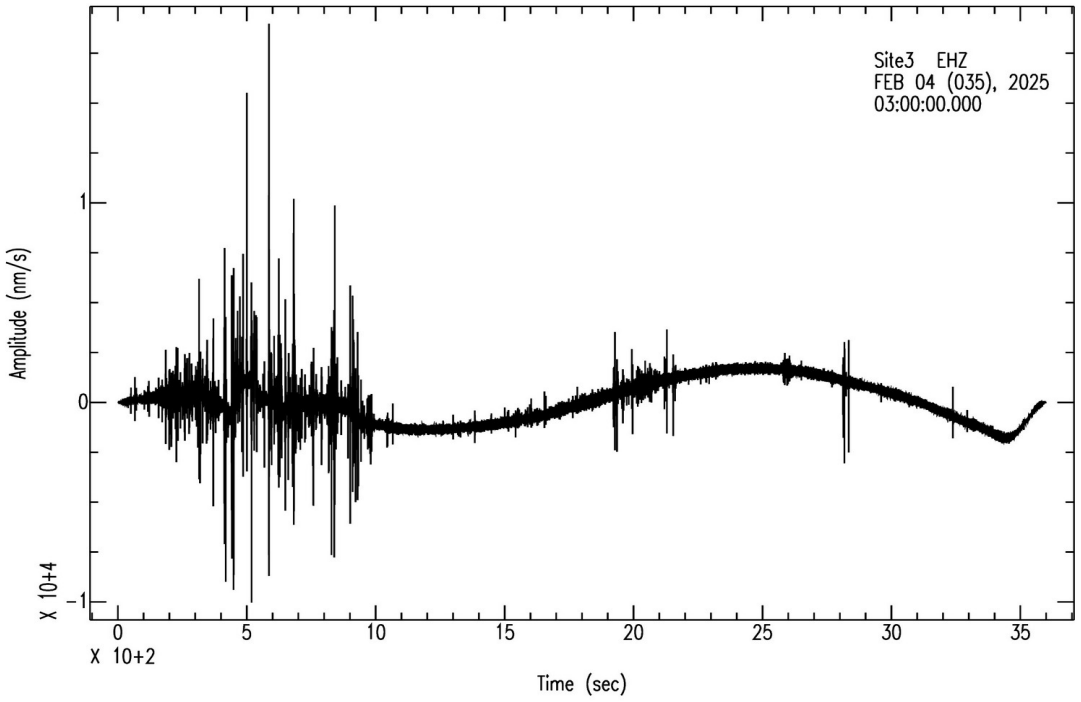

Figure 11: Seismic signals detected at Site 3, located 1500 meters from the well, during perforation gunfire.

3.3 Background Noise Analysis and Signal Attenuation:

Seismic monitoring faces challenges such as poor signal-to-noise ratio (SNR) due to high background noise and operational vibrations, which hinder the detection of weak signals. Seismic signal attenuation increases with distance from the well, with the highest peak displacement recorded at Site1 and weaker signals at Sites 2 and 3 due to energy loss in soft soils. We used the Geopsy tool (Le Pichon, 2009) with the Nakamura technique to analyze local noise activity, H/V estimates, and noise PSD spectrum at sites 2 and 3.

To improve seismic monitoring accuracy in hydraulic fracturing, expanding the sensor array, using broadband seismometers, and applying advanced data processing techniques are essential. Induced seismicity from perforation gun fire at 4500 meters caused fracturing in surrounding rock, generating small-magnitude seismic signals, especially in cases where fluid injection

altered stress conditions, increasing pore pressure in faults and fractures, as suggested by Segall et al. (2015). These signals were most detectable at Site 1, near the perforation.

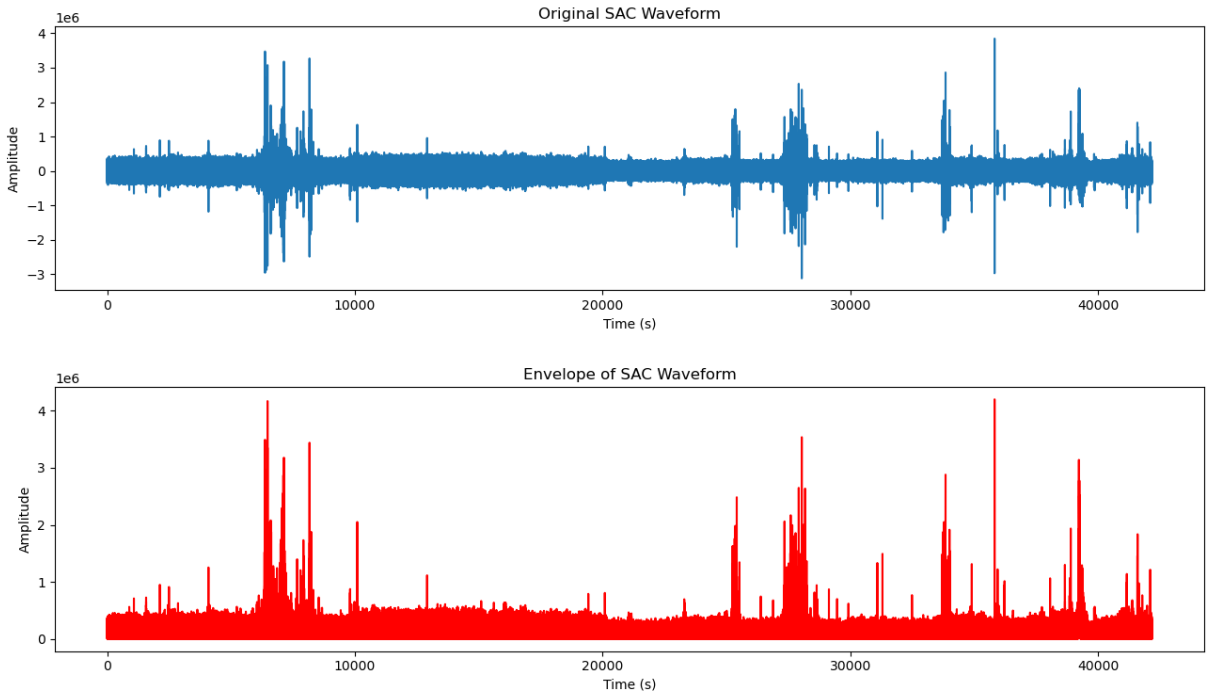

Figure 11a: The envelope of seismic signals detected at Site 3, 1500 meters from the well, during perforation gun firing.

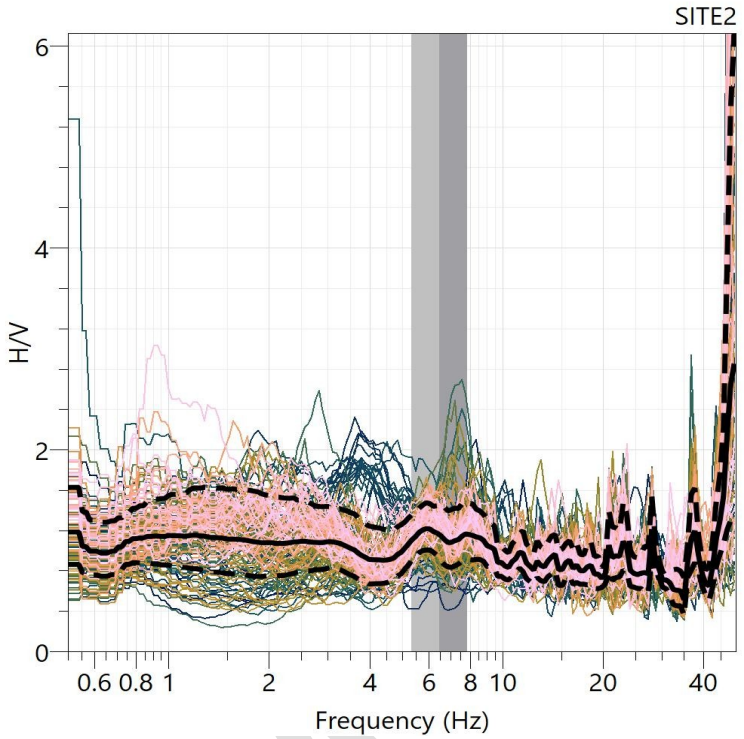

Figure 12: H/V analysis results indicating a resonance peak at a ratio of 1.5, suggesting the presence of a soft sediment layer beneath the site.

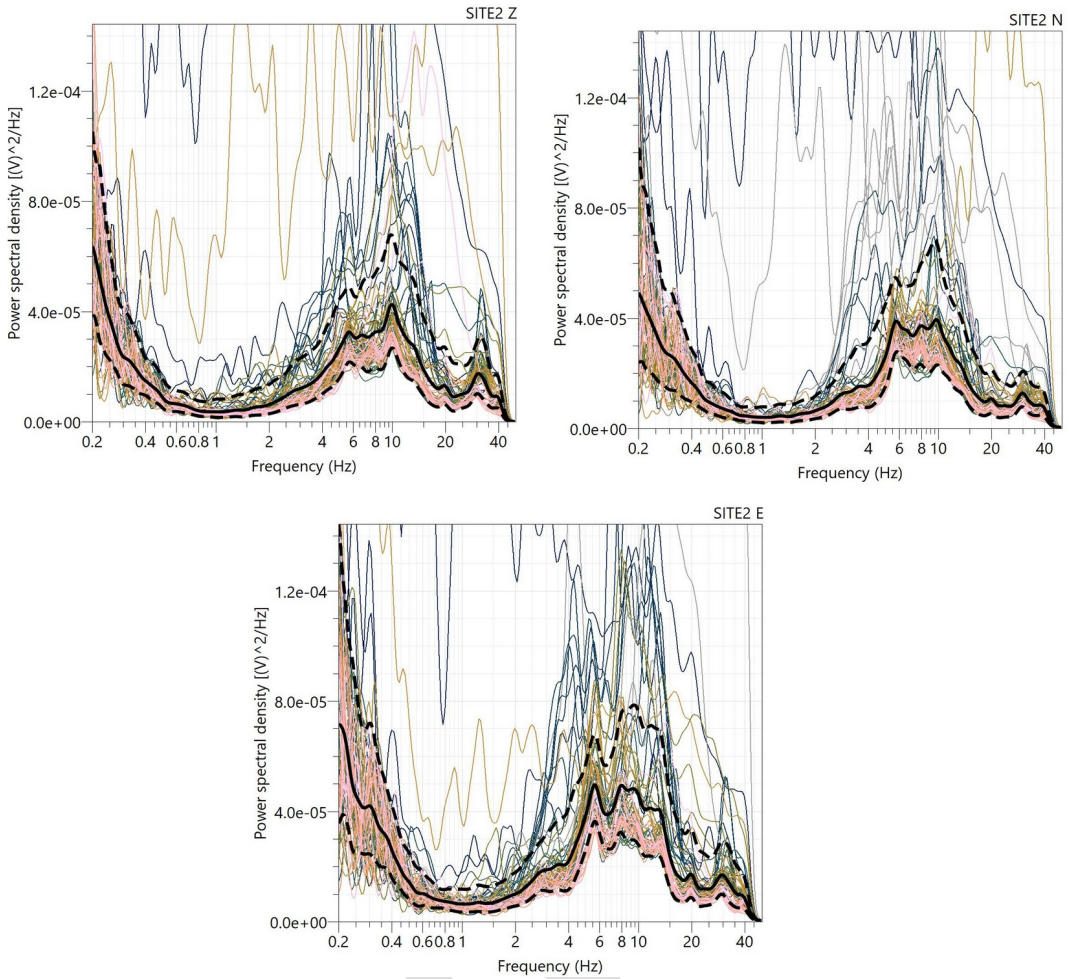

Figure 12b: Noise PSD results from three channels at Site 2 showing elevated noise levels, indicating site amplification in soft sediments.

Noise Power Spectral Density (PSD) results from Site 2 indicate elevated noise levels. Seismic signals weaken with distance, with greater attenuation observed at 500m and 1500m due to soft soil and alluvial deposits. Analyzing data from Sites2 and Site3 is more complex due to distance and other factors.

3.4 Ground Motion Distribution:

For an earthquake Mw 1.4 at a depth of 4500 meters, the peak ground acceleration (PGA) is low. Using an empirical model, the PGA in the yellow zone around the epicenter ranges from 0.01 to 0.151 cm/s². At sites Site2 and Site3, located farther from the epicenter (represented by the red star), the ground motion would be weaker, with PGA values closer to 0.01 cm/s². This weak ground motion is mostly imperceptible to people and detectable primarily by sensitive

instruments. These ground motion estimate results are similar to the magnitude estimates derived from seismic waveform analysis.

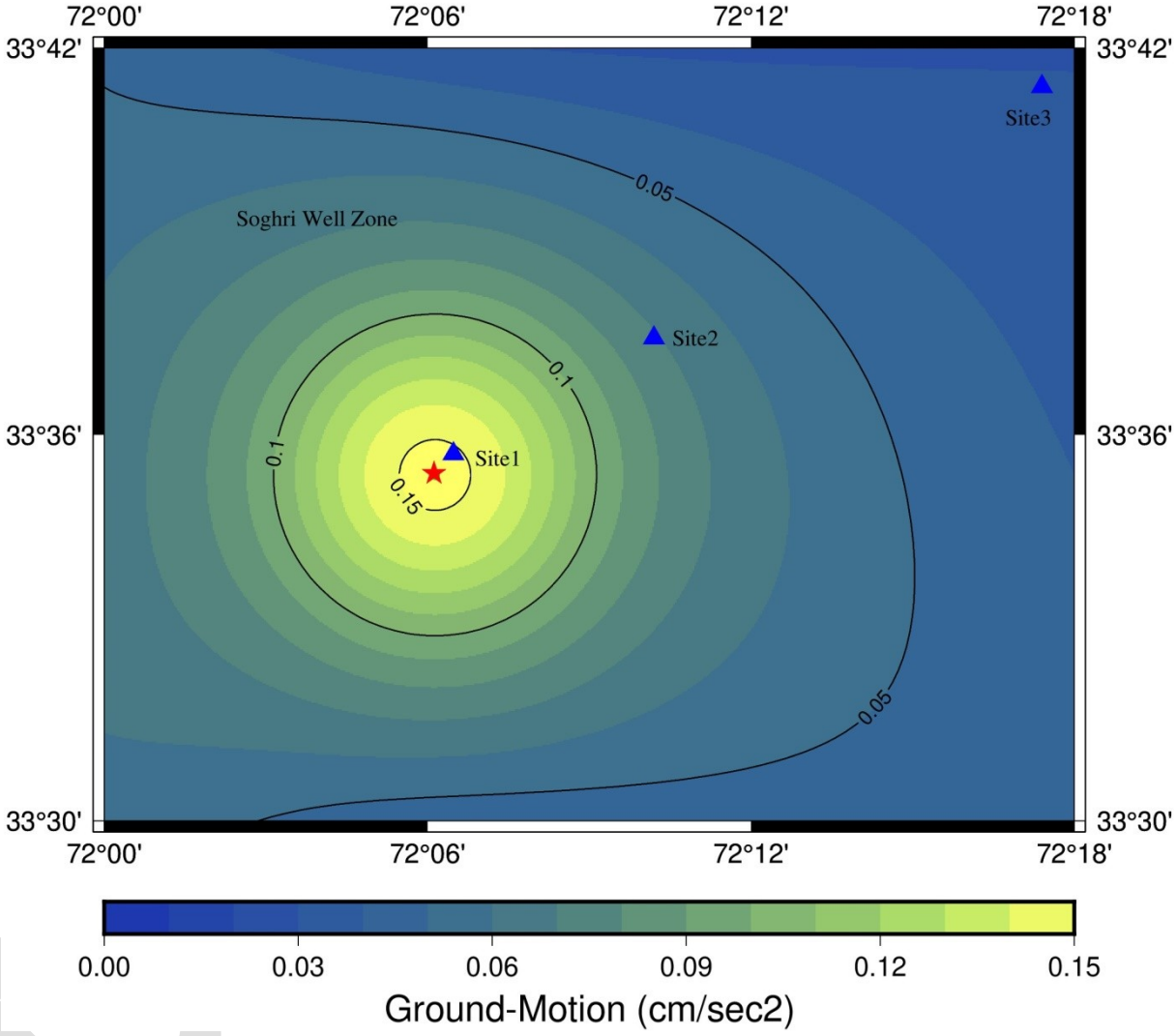

Figure 13: Ground Shaking Map, constructed using an empirical relation, showing the maximum shaking effect at 30 meters and negligible shaking at 1500 meters.

4. Discussion

This study introduces a novel approach to seismological monitoring in Pakistan, utilizing advanced instruments to detect micro-seismicity associated with perforation at an OGDCL well at a depth of 4500 meters. The technique effectively addresses challenges such as signal attenuation, poor signal-to-noise ratio (SNR), and background noise interference, surpassing traditional methods. It is particularly efficient at depths of 500m and 1500m, where soft soils significantly attenuate seismic signals. The results suggest that expanding the sensor array, deploying broadband seismometers, and integrating advanced signal processing techniques, such as machine learning-based noise filtering, could further enhance detection accuracy. Continuous seismic monitoring with these advanced methods is crucial for improving seismic risk assessments and supporting reservoir management efforts. Induced seismicity from the perforation gun fire caused rock fracturing, producing small-magnitude seismic signals, most detectable at Site 1, which is nearest to the perforation. Analysis of data from Sites 2 and 3 proved more complex due to their greater distance and other influencing factors. The rapid energy release from the perforation detonation triggered seismic events, with high pressure and temperature at this depth affecting the rock properties, including permeability, porosity, and fracture behavior. Ground shaking resulting from these events is a concern, highlighting the importance of monitoring both seismic data and well conditions. A comprehensive understanding of local geology and fault systems is essential to mitigate seismic risks. While induced seismicity was detected at a nearby station, the analysis was limited due to the reliance on data from only one station near the wellbore.

5. Conclusion

This study investigates seismic activity induced by perforation gun firing at the OGDCL Soghri Well (Rig-215) in Attock, Pakistan. The perforation process led to the detection of microseismic events, with the strongest signals recorded at Site 1, near the well. Minor peaks were observed at Sites 2 and 3, but due to signal attenuation and low SNR, it remains uncertain whether these were genuine seismic events or simply noise. Despite challenges such as poor SNR, signal attenuation, and limited sensor coverage, valuable data on induced seismicity was captured. A micro-earthquake with a magnitude of Mw 1.4 was recorded, and ground shaking maps revealed the strongest effects at 30 meters from the well, with negligible impact at 1500 meters. These ground motion estimates align with seismic waveform analysis for an Mw 1.4 event. The study emphasizes the importance of improving monitoring techniques, such as deploying broadband seismometers, expanding sensor networks, and utilizing advanced signal processing. Future

research should focus on enhancing seismic network coverage and adopting more sophisticated data analysis methods to improve seismic risk assessments and reservoir management. Induced seismicity from perforation gun fire at 4500 meters typically produces small-magnitude events, ranging from Mw 0.2 to 1.4, with most events falling below magnitude 2. The signals from perforation gun fire, characterized by high-frequency, short-duration waves, differ from natural earthquakes but can overlap with anthropogenic noise. These microseismic events are generally localized around the wellbore and are influenced by factors such as reservoir size, shot frequency, and local geology. However, they could trigger further seismic activity if reservoir pressure increases or if nearby faults are reactivated, as indicated by Segall et al. (2015), who suggest that fluid injection can reduce fault friction and potentially trigger earthquakes.

Acknowledgement

We thank OGDCL for granting access to the well site and providing logistical support. Special thanks to the field staff at the OGDCL well for assisting the PMD team during the sensor deployment. The seismology tools used in this study, as well as the maps constructed, were created using the latest GMT 6.5 tool. We acknowledge the developers and providers of these tools.

References

1. Bard, P.-Y., and SESAME Team. (2004). *Geopsy: Software for seismic noise analysis*. Retrieved from http://www.geopsy.org.
2. Beyreuther, M., Behr, Y., Krischer, L., Megies, T., Scherbaum, F., & Wetzel, H. (2010). ObsPy: A Python Toolbox for Seismology. *Seismological Research Letters, 81*(3), 530-533.
3. Goldstein, P., & Snoke, J. A. (2005). The Seismic Analysis Code (SAC) and its application to seismological research. *Seismological Research Letters, 76*(4), 485-493.
4. Le Pichon, A., & Dorbath, L. (2009). GeoPSY: Software for Seismic Processing and Interpretation. Proceedings of the European Geosciences Union (EGU) General Assembly 2009, Vienna, Austria.
5. Ottemöller, L., Voss, P.H., and Havskov, J. (2021). SEISAN Earthquake Analysis Software for Windows, Solaris, Linux, and macOS, Version 12.0. University of Bergen.
6. Kanamori, H. (1977). The energy release in great earthquakes. *Journal of Geophysical Research, 82*(20), 2981–2987.
7. Nakamura, Y. (1989). A method for dynamic characteristics estimation of subsurface using microtremor on the ground surface. *Quarterly Report, Technical Research Institute, 30*(1), 25–33.
8. Segall, P., & Lu, S. (2015). Earthquake triggering by fluid injection. *Seismological Research Letters, 86*(4), 1393–1405.
9. Wessel, P., Scharroo, R., Smith, W. H. F., & Luis, J. F. (2019). The Generic Mapping Tools (GMT) version 6. *Geochemistry, Geophysics, Geosystems*, *20*(11), 5556-5564.